Original Article

Cancer detection in patients with prostate-specific antigen levels within the grey zone: can synthetic magnetic resonance imaging aid in the differentiation between prostate cancer and noncancerous lesions?

Wenxin Cao[1#], Jinhua Lin[2#], Yanling Chen[1#], Jian Ling[3], Tiebao Meng[4], Zhihua Wen[1], Chuanmiao Xie[4], Long Qian[5], Yan Guo[1], Weijing Zhang[4], Huanjun Wang[1]

[1]Department of Radiology, The First Affiliated Hospital of Sun Yat-sen University, Guangzhou, China; [2]Department of Interventional Ultrasound, The First Affiliated Hospital of Sun Yat-sen University, Guangzhou, China; [3]Department of Radiology, The Eastern Hospital of The First Affiliated Hospital of Sun Yat-sen University, Guangzhou, China; [4]Department of Radiology, Sun Yat-sen University Cancer Center, Guangzhou, China; [5]Department of Biomedical Engineering, College of Engineering, Peking University, Beijing, China

Contributions: (I) Conception and design: W Cao, J Lin, Y Chen; (II) Administrative support: Y Guo, W Zhang, H Wang; (III) Provision of study materials or patients: J Ling, T Meng, Z Wen, C Xie, L Qian, Y Guo, W Zhang, H Wang; (IV) Collection and assembly of data: W Cao, J Lin, Y Chen, J Ling, Z Wen, L Qian; (V) Data analysis and interpretation: W Cao, J Lin, Y Chen, J Ling; (VI) Manuscript writing: All authors; (VII) Final approval of manuscript: All authors.

[#]These authors contributed equally to this work as co-first authors.

Correspondence to: Yan Guo, MD, PhD. Department of Radiology, The First Affiliated Hospital of Sun Yat-sen University, 58 Zhongshan Road 2, Guangzhou 510080, China. Email: gyan@mail.sysu.edu.cn; Weijing Zhang, MD, PhD. Department of Radiology, Sun Yat-sen University Cancer Center, 651 Dongfeng East Road, Guangzhou 510060, China. Email: zhangwj@sysucc.org.cn; Huanjun Wang, MD, PhD. Department of Radiology, The First Affiliated Hospital of Sun Yat-sen University, 58 Zhongshan Road 2, Guangzhou 510080, China. Email: wanghj45@mail.sysu.edu.cn.

Background: The detection of prostate cancer (PCa) via conventional magnetic resonance imaging (MRI) in patients with prostate-specific antigen (PSA) levels within the grey zone remains challenging. Whether synthetic MRI can provide supplementary benefits for the accurate diagnosis of PCa in this specific population is still unknown. This study aims to investigate the diagnostic performance of synthetic MRI for differentiating PCa lesions from noncancerous lesions in patients with PSA levels within the grey zone (4–10 ng/mL).

Methods: Clinical and MRI data, including synthetic MRI data of patients suspected of having PCa between August 2020 and August 2022, were retrospectively collected from The First Affiliated Hospital of Sun Yat-sen University and Sun Yat-sen University Cancer Center. Patients with PSA levels ranging from 4–10 ng/mL were enrolled. Pathology was obtained either from transrectal ultrasound-guided biopsy or radical prostatectomy. Regions of interest were manually drawn by two independent radiologists, and the values of quantitative parameters, including longitudinal relaxation time (T1), transverse relaxation time (T2), proton density (PD), and apparent diffusion coefficient (ADC), were separately measured. Interobserver agreement was evaluated using the interclass correlation coefficient (ICC). The differences in quantitative parameter values between PCa and noncancerous lesions were assessed using an independent sample *t*-test or the Mann-Whitney *U* test. Receiver operating characteristic curve analysis was performed to evaluate the diagnostic performance of each parameter (T1, T2, PD, and ADC values), as well as their combination. P<0.05 indicated statistical significance.

Results: A total of 130 patients were enrolled in this study, with a mean age of 67.32±8.87 years. The interobserver agreement of all the T1, T2, PD, and ADC values was classified as good or above (ICC =0.60–1.00). The means of the T1, T2, PD, and ADC values were significantly different between PCa

and noncancerous lesions (P=0.022, P<0.001, P=0.035, P<0.001, respectively). Notably, the ADC value demonstrated superior diagnostic performance compared to that of the other parameters, with an area under the curve (AUC) of 0.854 [95% confidence interval (CI): 0.781–0.909]. The combination of T1, T2, PD, and ADC values had a greater diagnostic performance (AUC =0.853, 95% CI: 0.781–0.909) than the T1 (AUC =0.622), T2 (AUC =0.721), or PD (AUC =0.608) values for differentiating PCa lesions from non-cancerous lesions. However, compared to the difference in the ADC value, no significant difference was found (P=0.982).

Conclusions: Quantitative parameters, including T1, T2, and PD, derived from synthetic MRI can be applied to differentiate PCa lesions from noncancerous lesions in patients with PSA levels within the grey zone. However, when these parameters were combined with the ADC, the diagnostic performance did not improve compared to that with the ADC value alone.

Keywords: Prostate cancer (PCa); prostate-specific antigen (PSA); grey zone; synthetic magnetic resonance imaging (synthetic MRI)

Submitted May 21, 2024. Accepted for publication Nov 01, 2024. Published online Nov 29, 2024.
doi: 10.21037/qims-24-1014
View this article at: https://dx.doi.org/10.21037/qims-24-1014

Introduction

Prostate cancer (PCa) is the second most common malignancy worldwide and also the fifth leading cause of global cancer death among men in 2022, which seriously threatens male health (1). Multiple PCa risk stratification tools, which consist of biomarkers based on blood and urine, risk calculators and magnetic resonance imaging (MRI), are applied to early screening, detection and diagnosis of PCa in current researches and guidelines (2-4). The prostate-specific antigen (PSA) test, which serves as the primary screening method, significantly contributes to the early detection of PCa (5-7). However, the specificity of PSA is widely considered low (8), especially when it is located in the grey zone at 4–10 ng/mL, since it can also result from various clinical conditions such as prostatitis, benign prostatic hyperplasia, digital rectal examination (DRE), transurethral examinations and so on. Therefore, PCa screening by PSA test is still debated (9). The limitation may lead to overdiagnosis, potentially causing unnecessary anxiety for patients, as well as the unnecessary biopsy or overtreatment. About up to 80% of biopsies are unnecessary for this population. Though some researchers have proposed that PSA density (PSAD) can assist in differentiating prostatitis and PCa in patients with PSA >4 ng/mL (10), there are still some limitations due to the fact that measurements of PSA and prostate volume are not standard and nor stable. Hence, detecting and screening PCas among this group of patients remain significant clinical challenges.

Multiparametric MRI (mpMRI), including T1, T2, diffusion-weighted imaging (DWI), and dynamic contrast enhancement (DCE), is the presently recommended imaging method for the diagnosis of prostate diseases, which promotes the early detection of intermediate/high-risk PCa cases (11,12). Prostate Imaging Reporting and Data System (PI-RADS) has been released to standardize the acquisition and interpretation of mpMRI images, which is now wildly used in the world (13,14). However, the subjectivity of each radiologist may influence the image interpretation and lead to false-positive results. There are still significant difficulties in differential diagnosis still exist for patients with a PSA level in the grey zone, especially when PSA combined with atypical MRI findings. Previous research indicates that the apparent diffusion coefficient (ADC) value from mpMRI demonstrates excellent performance in the detection and differential diagnosis of PCa, offering a quantitative representation of histopathological changes of prostate (15-18). The detection effectiveness of quantitative ADC values for PCa in this specific population needs further validation.

Synthetic MRI is an innovative quantitative MRI technique that utilizes a multidynamic multiecho (MDME) sequence to acquire absolute quantitative relaxation maps, including T1, T2, and proton density (PD), only in a single scan. It alternately acquires signals for each slice using different echo times and saturation delays. After a single scan, it can obtain the R1 and R2 image relaxation matrix of tissue, as well as the PD mapping. It relies on R1 and R2 to generate

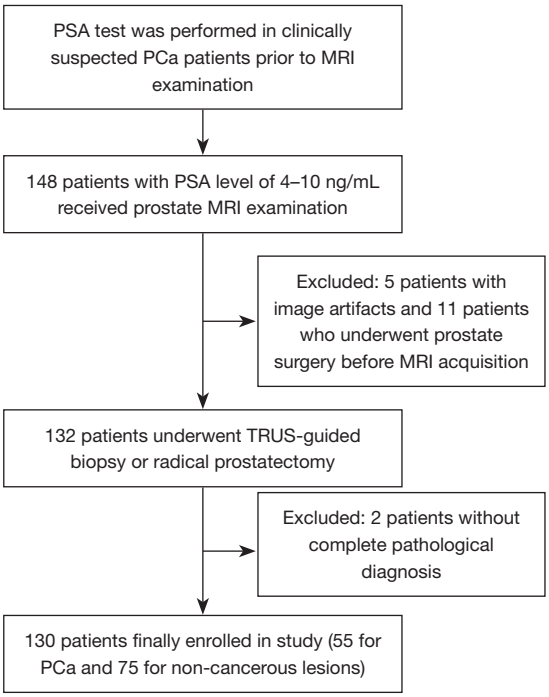

Figure 1 The flowchart of patients' selection. PSA, prostate-specific antigen; PCa, prostate cancer; MRI, magnetic resonance imaging; TRUS, transrectal ultrasound.

T1 mapping and T2 mapping, and then automatically reconstructs any contrast-weighted images. The image contrast acquired is dependent on the pixel values in the synthetic images, rather than the signal intensity changes produced by different tissue components in conventional MRI (19,20). This technique enables objective quantification of the biophysical characteristics of lesions and provides more objective data (21). Several studies have reported that quantitative parameters derived from synthetic MRI can assist in the diagnosis of diverse diseases including cancers and noncancerous diseases (20,22-26). Moreover, synthetic MRI has also been applied in the diagnosis of PCa (27-31). Nevertheless, to the best of our knowledge, no existing studies exploring the potential utility of synthetic MRI in the differential diagnosis of prostate lesions in patients with PSA in the grey zone have been reported.

Therefore, the aim of this study was to investigate the diagnostic performance of synthetic MRI for differentiating benign and malignant prostate lesions among patients with PSA levels within the grey zone, and further assess whether the novel synthetic MRI is prior to conventional ADC value for increasing PCa detection and improving prognosis of these specific patients. We present this article in accordance with the STARD reporting checklist (available at https://qims.amegroups.com/article/view/10.21037/qims-24-1014/rc).

Methods

Patients

Clinical and MRI data were retrospectively collected from patients who were clinically suspected of having PCa at The First Affiliated Hospital of Sun Yat-sen University and Sun Yat-sen University Cancer Center between August 2020 and August 2022. All consecutively included patients underwent a serum PSA test and mpMRI examination, which included synthetic MRI and DWI, before treatment, and transrectal ultrasound (TRUS)-guided biopsy or radical prostatectomy was subsequently performed within the next two weeks. This was done to exclude the influence of other factors such as disease progression and drug treatment, ensuring that the imaging findings match the pathological examination as closely as possible. According to the pathologic results, patients were divided into two groups: the PCa group defined as having Gleason score (GS) ≥3+3 (Grade Group 1–5); the noncancerous prostatic lesion group, including prostatitis, benign prostatic hyperplasia, and other benign lesions. The study was conducted in accordance with the Declaration of Helsinki (as revised in 2013). The study was approved by the Institutional Review Board of the First Affiliated Hospital of Sun Yat-sen University and Sun Yat-sen University Cancer Center {No. [2023]094} and individual consent for this retrospective analysis was waived.

The inclusion criteria of the study were as follows: (I) total PSA level was within 4–10 ng/mL; (II) all patients received mpMRI examination, including synthetic MRI and DWI, prior to biopsy or radical prostatectomy; and (III) pathological findings were clear and complete. The exclusion criteria were as follows: (I) a history of treatments (medication, pelvic radiation, chemotherapy) or specialized examinations (DRE, transurethral instrument examination) before the PSA test and MRI examination; (II) previous prostate puncture or surgery, such as transurethral resection of prostate; (III) insufficient MRI data or poor quality of images; and (IV) a lack of pathological results. The flowchart of patient selection is shown in *Figure 1*.

MRI protocol

MR images of all patients from the two centres were

acquired using a 3.0 T MRI scanner (Signa Pioneer, GE, Milwaukee, WI, USA) equipped with an 8-channel body phased array coil. The full MRI protocol comprises conventional contrast-weighted images (including axial T1-weighted images, axial, coronal, and sagittal T2-weighted images), axial DWI, and axial synthetic MRI.

(I) Axial T1-weighted fast spin echo (FSE) images: [repetition time/echo time (TR/TE), 661/8 ms; slice thickness, 3 mm; field of view (FOV), 240 mm × 240 mm; matrix, 352×288; number of excitations (NEX), 2; acquisition duration, 1 min 43 s]. (II) Axial, coronal, and sagittal T2-weighted PROPELLER images: (TR, 2,300/2,300/2,200 ms; TE, 90/90/90 ms; slice thickness, 3/3/3 mm; FOV, 240 mm × 240 mm/260 mm × 260 mm/240 mm × 240 mm; matrix, 352×352/352×352/352×352; NEX, 3.00/2.25/2.00 times; acquisition duration, 2 min 33/19/07 s). (III) Axial DWI images with b values of 50, 1,000 and 1,500 s/mm^2 were obtained by a single-shot echo-planar sequence (TR, 5,837/5,975 ms; slice thickness, 3/3 mm; FOV, 260 mm × 130 mm; matrix, (128×80)/(128×64); NEX, (2/16)/16 times; acquisition duration, 5 min 21 s/4 min 53 s). (IV) Axial synthetic MRI used a 2D MDME sequence with the following parameters: TR, 4,000 ms; TE1, 15.6 ms, TE2, 93.4 ms; slice thickness, 4 mm; FOV, 220 mm × 286 mm; matrix, 320×256; NEX, 1 time; acquisition duration, 6 min 8 s.

ADC maps were automatically calculated and generated from the raw DWI dataset based on b values of 50 and 1,000 s/mm^2. The quantitative parameter maps (T1, T2 and PD maps) of synthetic MRI were converted and generated using GE postprocessing software (SyMRI7.2; Synthetic MR, Linköping, Sweden).

Image postprocessing and analysis

The raw MDME data were processed using SyMRI7.2 software provided by above vendor to obtain quantitative parameter maps of TI, T2, and PD. Additionally, the AD map, combined with the quantitative parameter maps of TI, T2, and PD, was imported into ITK-SNAP software (version 3.8.0, 2019; www.itksnap.org). Two independent radiologists (W.C. and Y.C., with 2 and 4 years of pelvic imaging experience) who were blinded to the clinical information and pathological results manually delineated regions of interest (ROIs) in consecutive sections of each lesion on quantitative parameter maps by referring to the pelvic imaging. Simultaneously, quantitative parameters, including T1, T2, PD, and ADC values, were measured. All ROIs were drawn along the margin of the lesions encompassing the lesion areas as much as possible while excluding image artifacts, calcification, suspected hemorrhage, cysts, etc. Typical lesions were included in the analysis if there were multiple lesions. In instances where disagreements emerged, a consensus was reached after discussion with a senior radiologist (H.W.) with 14 years of pelvic imaging experience. Finally, the average T1, T2, PD, and ADC values were automatically calculated in the ROIs for each participant. The average values from the two radiologists were used for analysis.

Histopathological standards

The gold standard was based on the pathological examination of specimens obtained from radical prostatectomy and TRUS-guided biopsy. Before puncture operation, the prostate magnetic resonance images of patients would be read regularly by the same doctor with at least 10 years of prostate biopsy experience in interventional ultrasound department. Afterward, specimens of 12 cores including targeted suspicious lesions were successfully obtained. When patients underwent both puncture and radical prostatectomy, the pathological specimen from the radical prostatectomy was selected as the definitive reference standard. Based on the pathological results, the histopathological types were categorized into PCa (GS ≥3+3, Grade Group 1–5) and noncancerous lesions, which included benign prostatic hyperplasia, prostatitis, and other benign lesions.

Statistical analysis

Statistical Package for Social Sciences (SPSS) software (version 27.0, IBM, Armonk, NY, USA) was used for statistical analysis. The normality and homoscedasticity of the counting data were tested, and normally distributed count data were expressed as the mean ± standard deviation. The differences between PCa and noncancerous lesions were compared via an independent sample *t*-test (two-tailed). Otherwise, the data were expressed as medians (first quartile, third quartile), and the two-tailed Mann-Whitney *U* test was used for intergroup comparisons. Interobserver agreement was evaluated by using the interclass correlation coefficient (ICC). The interobserver reliability was classified as poor (ICC <0.4), moderate (ICC =0.4–0.59), good (ICC =0.6–0.74), or excellent (ICC =0.75–1.00). Multivariate logistic regression analysis was used to assess the combined

Table 1 Clinical data and lesion characteristics of patients enrolled in this study (n=130)

Parameters	PCa (n=55)	Non-PCa (n=75)	P value
Age (years)	70.09±6.66	65.29±9.74	0.001
TPSA (ng/mL)	7.26 (5.89, 8.46)	6.76 (4.98, 8.03)	0.839
FPSA (ng/mL)	1.04 (0.71, 1.61)	1.12 (0.73, 1.57)	0.169
FPSA/TPSA	0.14 (0.10, 0.26)	0.17 (0.13, 0.25)	0.105
Location of lesion			
PZ	42	18	
TZ	13	57	
Type of specimen			
TRUS-guided biopsy	16	62	
Radical prostatectomy	39	13	
ISUP GG and GS			
Benign tissue	–	75	
Grade 1 (3+3)	4	–	
Grade 2 (3+4)	24	–	
Grade 3 (4+3)	15	–	
Grade 4 (4+4)	9	–	
Grade 5 (>4+4)	3	–	

Data are expressed as mean ± standard deviation or median (first quartile, third quartile). PCa, prostate cancer; non-PCa, non-cancerous lesions, including benign prostatic hyperplasia, prostatitis, etc.; TPSA, total prostate-specific antigen; FPSA, free prostate-specific antigen; TZ, transitional zone; PZ, peripheral zone; TRUS, transrectal ultrasound; ISUP, International Society of Urological Pathology; GG, Grade Group; GS, Gleason Score.

diagnostic performance of the parameters. Both the receiver operating characteristic (ROC) curve and the calculation of each area under the curve (AUC) were sequentially performed by using the MedCalc (version 19.2; Ostend, Belgium; www.medcalc.org) program. Therefore, the diagnostic performance of the T1, T2, PD, and ADC values and their combination in distinguishing PCa lesions from noncancerous lesions were assessed. The optimal cut-off was determined by the Youden-index. Areas under the curve (AUCs) were compared using the Delong test. $P<0.05$ was considered to indicate a statistically significant difference.

Results

Patient characteristics

The detailed clinical data of the eligible patients can be found in *Table 1*. A total of 130 patients (101 from the First Affiliated Hospital of Sun Yat-sen University and 29 from Sun Yat-sen University Cancer Center) with 130 prostate lesions were ultimately included in the study. The mean age of the patients was 67.32±8.87 years, and the mean total PSA (TPSA) level was 6.93 (5.61–8.25) ng/mL. According to adopted the pathological results, 42.3% (55 out 130) of the patients were confirmed to have PCa, and 57.7% (75 out of 130) had noncancerous lesions such as prostatitis, benign prostatic hyperplasia. There was a significant difference in the age distribution between patients with PCa and patients with noncancerous lesions ($P<0.05$), while the overall distributions of TPSA, free PSA (FPSA), and the PSA ratio (FPSA/TPSA) were not significantly different ($P=0.839$, 0.169, 0.105, respectively).

Interobserver agreement

The interobserver agreement of the quantitative parameters (T1, T2, PD, and ADC value) measured by the two observers was considered good and above, with ICCs of 0.876, 0.947,

Table 2 Consistency analysis between the two-reader

Parameters	Reader 1	Reader 2	ICC
T1 (ms)	1,351.02 (1,236.13, 1,450.99)	1,358.87 (1,238.56, 14,47.36)	0.876
T2 (ms)	90.51 (81.16, 103.14)	90.71 (81.19, 103.55)	0.947
PD (pu)	81.60 (79.81, 83.51)	81.69 (79.70, 83.48)	0.647
ADC ($\times10^{-6}$ mm^2/s)	1,086.80±237.19	1,089.79±234.37	0.981

Data are expressed as mean ± standard deviation or median (first quartile, third quartile). Reliability was considered poor (ICC, <0.40), fair (ICC, 0.4–0.59), good (ICC, 0.60–0.74), or excellent (ICC, 0.75–1.00). PD, proton density; ADC, apparent diffusion coefficient; ICC, interclass correlation coefficient.

Table 3 Comparisons of quantitative parameters derived from synthetic MRI and ADC value

Parameters	PCa	Non-PCa	P value
T1 (ms)	1,314.12±138.07	1,378.94±180.17	0.022
T2 (ms)	85.51 (78.97, 90.52)	97.27 (84.60, 106.98)	<0.001
PD (pu)	80.93 (80.20, 82.60)	82.32 (79.41, 84.09)	0.035
ADC ($\times10^{-6}$ mm^2/s)	937.07±173.21	1203.13±204.02	<0.001

Data are expressed as mean ± standard deviation or median (first quartile, third quartile). MRI, magnetic resonance imaging; ADC, apparent diffusion coefficient; PCa, prostate cancer; Non-PCa: non-cancerous prostatic lesions, including benign prostatic hyperplasia, prostatitis, etc.; PD, proton density.

0.647, and 0.981, respectively, shown in *Table 2*.

Quantitative parameters derived from synthetic MRI and DWI sequences

Significant differences were observed in the mean T1, T2, PD, and ADC values between the cancer group and the noncancerous lesion group (P<0.05), with lower values consistently found in the PCa group (*Table 3*). *Figures 2*,*3* show the MR findings of patients with PCa and benign lesions, respectively.

Diagnostic performance of MRI parameters in differentiating PCa from noncancerous lesions

The results of the ROC analysis are shown in *Table 4* and *Figure 4*. The ADC value demonstrated the highest AUC (0.854; 95% CI: 0.781–0.909) for differentiating PCa from noncancerous lesions. The optimal cut-off value was determined to be 1,036.22×10^{-6} mm^2/s, with a sensitivity of 80% and a specificity of 80%. The AUC of the combination of T1, T2 and PD was 0.731 (95% CI: 0.647–0.805), which didn't show higher diagnostic performance compared with ADC value. Furthermore, the combination of T1, T2, PD and ADC values achieved the AUC of 0.853 (95% CI: 0.781–0.909), which significantly improved the diagnostic performance for distinguishing PCa compared to the individual values of T1, T2, and PD (AUC =0.622, 0.721, 0.608, all P<0.05), except for the ADC value (P>0.05).

Discussion

In this study, the results revealed that cancer lesions exhibited significantly lower T1, T2, PD and ADC values than benign prostate lesions in patients with PSA levels in the grey zone. These findings are consistent with previous findings that the T1 value, serving as an indicator of water and biomolecule content in tissues (32), can be used to distinguish PCa from noncancerous tissues (27); however, one study has reported that there is no statistically significant difference in T1 values between benign and malignant lesions in the peripheral zone of the prostate (33), suggesting that the diagnostic performance of the T1 value in prostate diseases still needs to be further explored.

In our study, significantly lower T2 value was also shown for PCa lesions than for noncancerous lesions for patients with PSA levels in the grey zone, which is consistent with the findings of several previous studies reporting that the

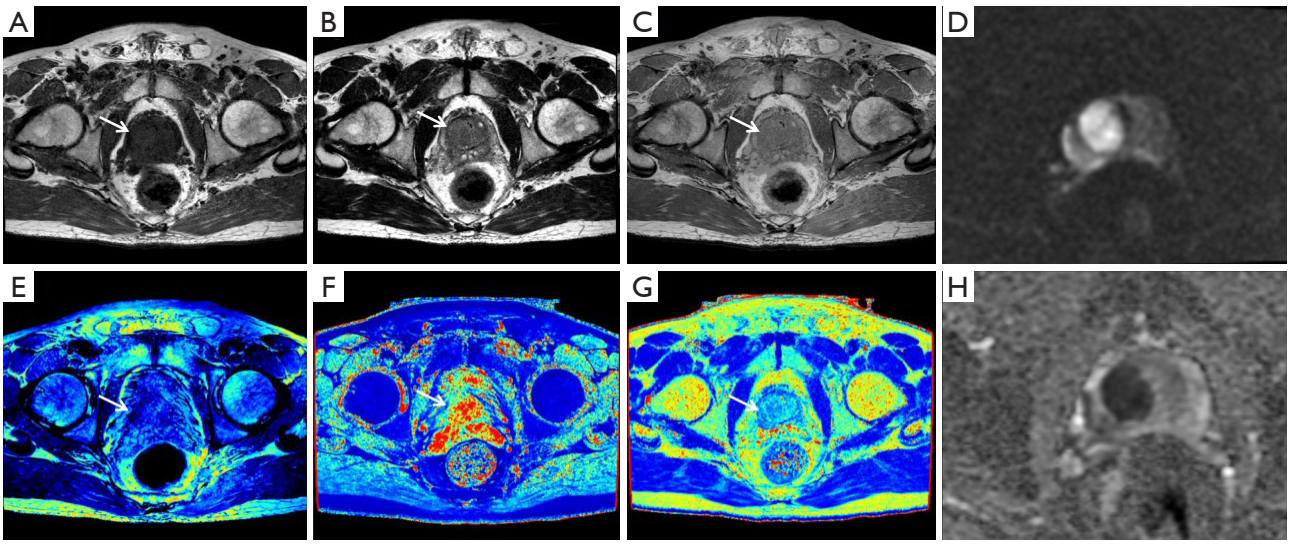

Figure 2 Prostate MR images of a 63-year-old man with PSA level is 9.41 (ng/mL). A lesion was found located in the right TZ (white arrow), which was pathologically confirmed to be PCa (GS 3+5). (A-C) T1-, T2- and PD-weighted images obtained from SyMRI all show a low-signal intensity focus in the right TZ. (D) Axial diffusion-weighted image (b=1,500 s/mm^2) demonstrates a high-signal intensity. This finding is corroborated by the (H) ADC map, which also reveals a low-signal intensity at the focus point corresponding to the location of the abnormal signal on the SyMRI scan. This abnormal signal is indicative of restricted diffusion. And the mean ADC value measured by the two radiologists was 862.31×10^{-6} mm^2/s. (E-G) SyMRI-derived T1, T2 and PD maps indicate that the mean T1, T2, and PD values of the lesion measured by the two radiologists were 1,377.34 ms, 85.52 ms and 82.38 pu, respectively. MR, magnetic resonance; PSA, prostate-specific antigen; TZ, transition zone; PCa, prostate cancer; PD, proton density; SyMRI, synthetic magnetic resonance imaging; ADC, apparent diffusion coefficient.

T2 relaxation time of PCa patients is significantly lower than that of noncancerous areas in patients with varied PSA levels (29,30,34-36). This might be because the proliferation of cancer cells in the prostate replaces relatively loose normal glandular tissue, resulting in a decrease in the T2 relaxation time in the corresponding area (37,38). We first applied this T2 value in the differentiation of prostate diseases in patients with PSA levels in grey zone, and the results suggested that the T2 value is highly feasible and reproducible for helping detect histopathological changes in prostate lesions regardless of PSA level. Similarly, Song *et al.* also found that T2 value have diagnostic performance comparable to that of ADC (AUC: 0.963 *vs.* 0.991), and can further distinguish low risk from intermediate/high risk PCa (30).

Additionally, we also observed that PD values were lower in cancer lesions than in noncancerous lesions among patients with PSA in the grey area. However, its diagnostic performance was lower than that of the T1 or T2 values. Similarly, a previous study conducted by Cui *et al.* (27) reported that PD was not significantly associated with distinguishing PCa from stromal hyperplasia nodules or from the normal peripheral zone; moreover, PSA levels were not analyzed in that study. However, another study argued that PD values have certain value in the detection of bone metastasis in PCa (39). Thus, the potential application of PD in the differential diagnosis of PCa, especially when patients have a PSA level within the grey zone, also remains to be validated.

Our results demonstrated that the diagnostic performance of a single ADC value outperformed that of the other parameters and was comparable to that of the combination of the ADC and synthetic MRI parameters. Recently, Gao *et al.* reported that the diagnostic model combining synthetic MRI (T2 + PD) with ADC value (AUC: 0.818) shows promise in differentiating low risk PCa and its risk upgrade (31). We have also observed similar results, confirming that synthetic MRI has positive significance in the diagnosis of PCa for patients in the grey zone, providing a radiological reference for decisions on biopsy and clinical treatment. However, it cannot be overlooked that a previous study conducted by Cai *et al.* (25) indicated

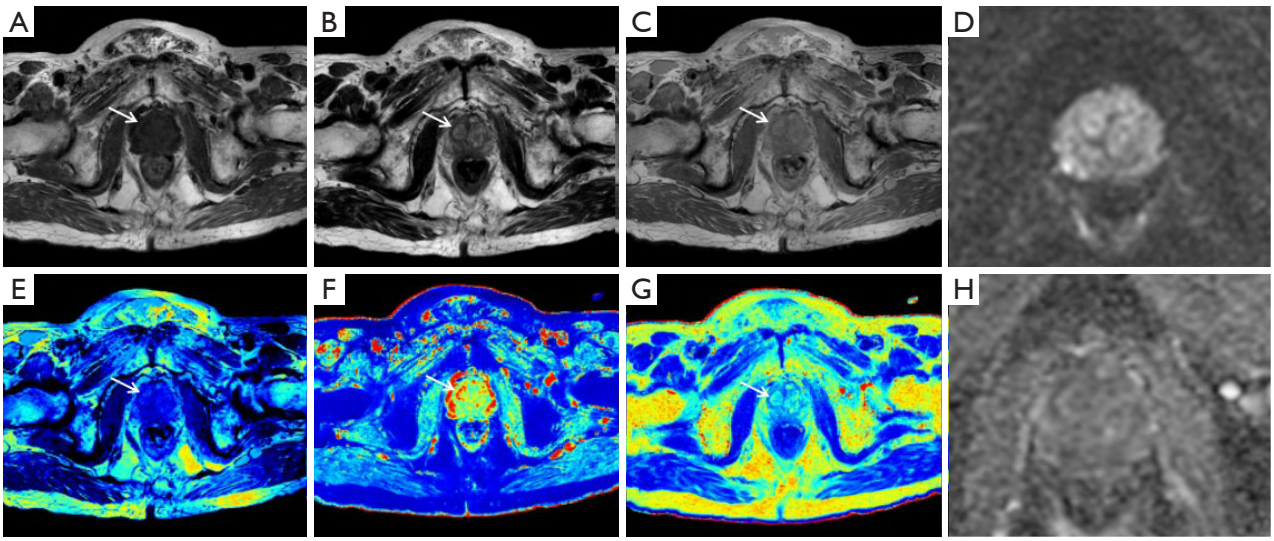

Figure 3 Prostate MR images of an 84-year-old man with PSA level of 7.28 ng/mL. A lesion was found located in the right TZ (white arrow), which was pathologically confirmed to be benign prostatic hyperplasia. (A-C) T1-, T2- and PD-weighted images were obtained from SyMRI. Both T2- and PD-weighted images show a slightly hyperintense signal in the right TZ. Both (D) axial diffusion-weighted image (b=1,500 s/mm^2) and ADC map (H) demonstrate no evidence of diffusion restriction with an intermediate-signal intensity at the focus point corresponding to the location of the abnormal signal on the SyMRI scan. And the mean ADC value measured by the two radiologists was 1,323.78×10^{-6} mm^2/s. (E-G) SyMRI-derived T1, T2 and PD maps indicate that the mean T1, T2, and PD values measured by the two radiologists were 1,589.05 ms, 97.23 ms and 85.20 pu, respectively. MR, magnetic resonance; PSA, prostate-specific antigen; TZ, transition zone; SyMRI, synthetic magnetic resonance imaging; PD, proton density; ADC, apparent diffusion coefficient.

Table 4 Diagnostic performance of T1, T2, PD, and ADC values in differentiating PCa from non-cancerous lesions

Parameters	AUC (95% CI)	Cutoff value	Sensitivity (%)	Specificity (%)
T1 (msec)	0.622 (0.532, 0.705)	1,404.88	83.64	48
T2 (msec)	0.721 (0.636, 0.796)	95.59	85.45	57.33
PD (pu)	0.608 (0.519, 0.693)	82.52	76.36	48
ADC (×10^{-6} mm^2/s)	0.854 (0.781, 0.909)	1,036.22	80	80
T1 + T2 + PD	0.731 (0.647, 0.805)		81.82	57.33
T1 + T2 + PD + ADC	0.853 (0.781, 0.909)		83.64	74.67

PD, proton density; ADC, apparent diffusion coefficient; PCa, prostate cancer; AUC: area under the curve; CI, confidence interval.

that synthetic MRI was slightly inferior to the ADC value in differentiating high-grade from low-grade bladder cancer. This suggests that mpMRI still plays an irreplaceable role in the detection of PCa in the PSA grey zone population (40). Other imaging methods such as prostate-specific membrane antigen positron emission tomography/computed tomography (PSMA PET-CT) and ultrasound also offer benefits in the diagnosis of PCa. However, less attention was paid to PSA grey zone population, and the aforementioned imaging methods emphasized the combination with clinical indicators (41-44). Comparative studies on synthetic MRI with these imaging methods require further exploration and validation. Therefore, based on our research findings, we recommend considering ADC as a crucial factor in the diagnosis of prostate diseases in patients with PSA in the grey zone, as this approach further offers simplicity and improved accuracy in the diagnostic process.

Several limitations must be acknowledged in our study.

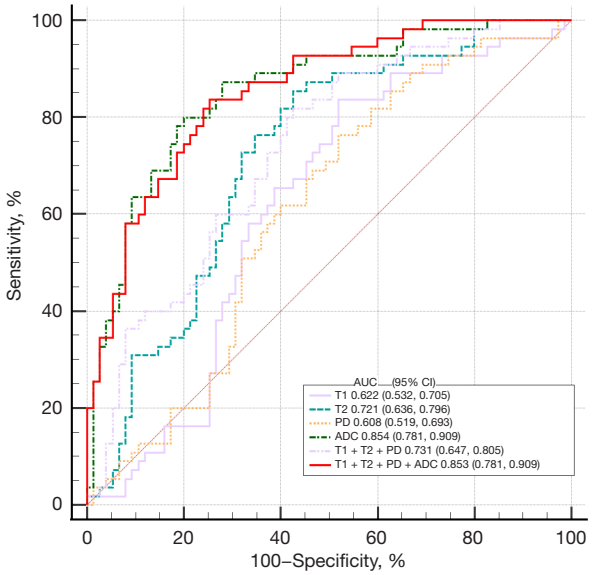

Figure 4 ROC curve analyses of the T1, T2, PD, ADC values, and their combination for differentiating PCa. The areas under the ROC curves for the mean T1, T2, PD and ADC values were 0.622, 0.721, 0.608, 0.854, 0.731 and 0.853, respectively. ROC, receiver operating characteristic; PD, proton density; ADC, apparent diffusion coefficient; CI, confidence interval; PCa, prostate cancer.

First, our retrospective study was limited by a relatively small sample size, although the data were collected from a dual-centre, and further prospective studies with larger sample sizes are still needed. Second, in this article, we only explored the diagnosis of benign prostatic lesions versus PCa (GS ≥3+3) rather than the issue of clinically significant PCa (csPCa) diagnosis as our study is merely a preliminary exploration of differential diagnosis for PCa. We believe that some clinically insignificant lesions (GS =3+3) should also be distinguished from benign prostatic lesions, as these lesions are also recommended for active follow-up and surveillance (45). The performance of synthetic MRI for the diagnosis of csPCa, and even ambiguous PI-RADS 3 lesions requires further in-depth exploration in the future. And it should be noted that the mean age of patients in the PCa group was significantly greater than that of patients in the noncancerous lesion group. These age differences may introduce variations in quantitative parameters (T1, T2, PD, and ADC values) between the prostate tissue itself and prostate lesions among patients in different age groups (5); such variations might impact the study results although they need to be further explored. Additionally, we did not delineate ROIs for multiple lesions, which might introduce bias into the study. Considering the potential impact of these factors, further prospective researches in multiple centers should aim to address these limitations for a more comprehensive analysis.

Conclusions

In conclusion, synthetic MRI is feasible and helpful for distinguishing PCa lesions from noncancerous lesions among patients with PSA levels in the grey zone. However, this approach cannot significantly improve the differential diagnostic performance of the ADC value. Thus, in clinical practice, we still recommend prioritizing the use of the ADC value for PCa screening in patients with PSA levels in grey zone.

Acknowledgments

The authors gratefully acknowledge the comprehensive language editing services provided by American Journal Experts.
Funding: This work was supported by the National Natural Science Foundation of China (Nos. 82372075, 82371911, 82071989) and the Natural Science Outstanding Youth Fund of Guangdong Province (No. 2024B1515020061).

Footnote

Reporting Checklist: The authors have completed the STARD reporting checklist. Available at https://qims.amegroups.com/article/view/10.21037/qims-24-1014/rc

Conflicts of Interest: All authors have completed the ICMJE uniform disclosure form (available at https://qims.amegroups.com/article/view/10.21037/qims-24-1014/coif). The authors have no conflicts of interest to declare.

Ethical Statement: The authors are accountable for all aspects of the work in ensuring that questions related to the accuracy or integrity of any part of the work are appropriately investigated and resolved. The study was conducted in accordance with the Declaration of Helsinki (as revised in 2013). The study was approved by the Institutional Review Board of The First Affiliated Hospital of Sun Yat-sen University and Sun Yat-sen University Cancer Center {No. [2023]094} and individual consent for this retrospective analysis was waived.

References

1. Bray F, Laversanne M, Sung H, Ferlay J, Siegel RL, Soerjomataram I, Jemal A. Global cancer statistics 2022: GLOBOCAN estimates of incidence and mortality worldwide for 36 cancers in 185 countries. CA Cancer J Clin 2024;74:229-63.
2. Osses DF, Roobol MJ, Schoots IG. Prediction Medicine: Biomarkers, Risk Calculators and Magnetic Resonance Imaging as Risk Stratification Tools in Prostate Cancer Diagnosis. Int J Mol Sci 2019;20:1637.
3. Mottet N, Bellmunt J, Bolla M, Briers E, Cumberbatch MG, De Santis M, et al. EAU-ESTRO-SIOG Guidelines on Prostate Cancer. Part 1: Screening, Diagnosis, and Local Treatment with Curative Intent. Eur Urol 2017;71:618-29.
4. Van Poppel H, Hogenhout R, Albers P, van den Bergh RCN, Barentsz JO, Roobol MJ. Early Detection of Prostate Cancer in 2020 and Beyond: Facts and Recommendations for the European Union and the European Commission. Eur Urol 2021;79:327-9.
5. Zhou CK, Check DP, Lortet-Tieulent J, Laversanne M, Jemal A, Ferlay J, Bray F, Cook MB, Devesa SS. Prostate cancer incidence in 43 populations worldwide: An analysis of time trends overall and by age group. Int J Cancer 2016;138:1388-400.
6. Culp MB, Soerjomataram I, Efstathiou JA, Bray F, Jemal A. Recent Global Patterns in Prostate Cancer Incidence and Mortality Rates. Eur Urol 2020;77:38-52.
7. Fenton JJ, Weyrich MS, Durbin S, Liu Y, Bang H, Melnikow J. Prostate-Specific Antigen-Based Screening for Prostate Cancer Evidence Report and Systematic Review for the US Preventive Services Task Force. JAMA 2018;319:1914-31.
8. Hugosson J, Roobol MJ, Månsson M, Tammela TLJ, Zappa M, Nelen V, et al. A 16-yr Follow-up of the European Randomized study of Screening for Prostate Cancer. Eur Urol 2019;76:43-51.
9. Beatrici E, Filipas DK, Stone BV, Labban M, Qian Z, Lipsitz SR, Lughezzani G, Buffi NM, Cole AP, Trinh QD. Clinical stage and grade migration of localized prostate cancer at diagnosis during the past decade. Urol Oncol 2023;41:483.e11-9.
10. Bruno SM, Falagario UG, d'Altilia N, Recchia M, Mancini V, Selvaggio O, Sanguedolce F, Del Giudice F, Maggi M, Ferro M, Porreca A, Sciarra A, De Berardinis E, Bettocchi C, Busetto GM, Cormio L, Carrieri G. PSA Density Help to Identify Patients With Elevated PSA Due to Prostate Cancer Rather Than Intraprostatic Inflammation: A Prospective Single Center Study. Front Oncol 2021;11:693684.
11. Qian Z, Chen YJ, Feldman J, Beatrici E, Filipas DK, Moore CM, Trinh QD, Kibel AS, Lipsitz SR, Cole AP. Prostate magnetic resonance imaging utilization and its relationship with advanced prostate cancer detection. Urol Oncol 2024;42:370.e1-7.
12. Mayer R, Simone CB 2nd, Turkbey B, Choyke P. Development and testing quantitative metrics from multi-parametric magnetic resonance imaging that predict Gleason score for prostate tumors. Quant Imaging Med Surg 2022;12:1859-70.
13. Turkbey B, Rosenkrantz AB, Haider MA, Padhani AR, Villeirs G, Macura KJ, Tempany CM, Choyke PL, Cornud F, Margolis DJ, Thoeny HC, Verma S, Barentsz J, Weinreb JC. Prostate Imaging Reporting and Data System Version 2.1: 2019 Update of Prostate Imaging Reporting and Data System Version 2. Eur Urol 2019;76:340-51.
14. Weinreb JC, Barentsz JO, Choyke PL, Cornud F, Haider MA, Macura KJ, Margolis D, Schnall MD, Shtern F, Tempany CM, Thoeny HC, Verma S. PI-RADS Prostate Imaging - Reporting and Data System: 2015, Version 2. Eur Urol 2016;69:16-40.
15. Maurer MH, Heverhagen JT. Diffusion weighted imaging of the prostate-principles, application, and advances. Transl Androl Urol 2017;6:490-8.
16. Vos EK, Kobus T, Litjens GJ, Hambrock T, Hulsbergen-van de Kaa CA, Barentsz JO, Maas MC, Scheenen TW. Multiparametric Magnetic Resonance Imaging for Discriminating Low-Grade From High-Grade Prostate Cancer. Invest Radiol 2015;50:490-7.
17. Yoshimitsu K, Kiyoshima K, Irie H, Tajima T, Asayama Y, Hirakawa M, Ishigami K, Naito S, Honda H. Usefulness of apparent diffusion coefficient map in diagnosing prostate carcinoma: correlation with stepwise histopathology. J Magn Reson Imaging 2008;27:132-9.
18. Xing P, Chen L, Yang Q, Song T, Ma C, Grimm R, Fu C, Wang T, Peng W, Lu J. Differentiating prostate

cancer from benign prostatic hyperplasia using whole-lesion histogram and texture analysis of diffusion- and T2-weighted imaging. Cancer Imaging 2021;21:54.
19. Gonçalves FG, Serai SD, Zuccoli G. Synthetic Brain MRI: Review of Current Concepts and Future Directions. Top Magn Reson Imaging 2018;27:387-93.
20. Hagiwara A, Warntjes M, Hori M, Andica C, Nakazawa M, Kumamaru KK, Abe O, Aoki S. SyMRI of the Brain: Rapid Quantification of Relaxation Rates and Proton Density, With Synthetic MRI, Automatic Brain Segmentation, and Myelin Measurement. Invest Radiol 2017;52:647-57.
21. Krauss W, Gunnarsson M, Andersson T, Thunberg P. Accuracy and reproducibility of a quantitative magnetic resonance imaging method for concurrent measurements of tissue relaxation times and proton density. Magn Reson Imaging 2015;33:584-91.
22. Hagiwara A, Hori M, Yokoyama K, Takemura MY, Andica C, Tabata T, Kamagata K, Suzuki M, Kumamaru KK, Nakazawa M, Takano N, Kawasaki H, Hamasaki N, Kunimatsu A, Aoki S. Synthetic MRI in the Detection of Multiple Sclerosis Plaques. AJNR Am J Neuroradiol 2017;38:257-63.
23. Meng T, He N, He H, Liu K, Ke L, Liu H, Zhong L, Huang C, Yang A, Zhou C, Qian L, Xie C. The diagnostic performance of quantitative mapping in breast cancer patients: a preliminary study using synthetic MRI. Cancer Imaging 2020;20:88.
24. Kazama T, Takahara T, Kwee TC, Nakamura N, Kumaki N, Niikura N, Niwa T, Hashimoto J. Quantitative Values from Synthetic MRI Correlate with Breast Cancer Subtypes. Life (Basel) 2022.
25. Cai Q, Wen Z, Huang Y, Li M, Ouyang L, Ling J, Qian L, Guo Y, Wang H. Investigation of Synthetic Magnetic Resonance Imaging Applied in the Evaluation of the Tumor Grade of Bladder Cancer. J Magn Reson Imaging 2021;54:1989-97.
26. Boudabbous S, Neroladaki A, Bagetakos I, Hamard M, Delattre BM, Vargas MI. Feasibility of synthetic MRI in knee imaging in routine practice. Acta Radiol Open 2018;7:2058460118769686.
27. Cui Y, Han S, Liu M, Wu PY, Zhang W, Zhang J, Li C, Chen M. Diagnosis and Grading of Prostate Cancer by Relaxation Maps From Synthetic MRI. J Magn Reson Imaging 2020;52:552-64.
28. Park SB. Quantitative relaxation maps from synthetic MRI for prostate cancer. Acta Radiol 2022;63:982-3.
29. Arita Y, Akita H, Fujiwara H, Hashimoto M, Shigeta K, Kwee TC, Yoshida S, Kosaka T, Okuda S, Oya M, Jinzaki M. Synthetic magnetic resonance imaging for primary prostate cancer evaluation: Diagnostic potential of a non-contrast-enhanced bi-parametric approach enhanced with relaxometry measurements. Eur J Radiol Open 2022;9:100403.
30. Song N, Wang T, Zhang D, Wang Z, Zhang SR, Yu J, Cai L, Ma AL, Zhang Q, Chen ZQ. The value of relaxation time quantitative technique from synthetic magnetic resonance imaging in the diagnosis and invasion assessment of prostate cancer. Zhonghua Yi Xue Za Zhi 2022;102:1093-9.
31. Gao Z, Xu X, Sun H, Li T, Ding W, Duan Y, Tang L, Gu Y. The value of synthetic magnetic resonance imaging in the diagnosis and assessment of prostate cancer aggressiveness. Quant Imaging Med Surg 2024;14:5473-89.
32. Gelman N, Ewing JR, Gorell JM, Spickler EM, Solomon EG. Interregional variation of longitudinal relaxation rates in human brain at 3.0 T: relation to estimated iron and water contents. Magn Reson Med 2001;45:71-9.
33. Cao H, Xu W, Xu Y, Rong X, Xiao X, Feng H, Wang X, Wang L, Qi T, Zhang L. Value of synthetic MRI quantitative parameters in preprocedural evaluation for TRUS/MRI fusion-guided biopsy of the prostate. Prostate 2023;83:1089-98.
34. Liu W, Turkbey B, Sénégas J, Remmele S, Xu S, Kruecker J, Bernardo M, Wood BJ, Pinto PA, Choyke PL. Accelerated T2 mapping for characterization of prostate cancer. Magn Reson Med 2011;65:1400-6.
35. Wu LM, Chen XX, Xuan HQ, Liu Q, Suo ST, Hu J, Xu JR. Feasibility and preliminary experience of quantitative T2* mapping at 3.0 T for detection and assessment of aggressiveness of prostate cancer. Acad Radiol 2014;21:1020-6.
36. Yu AC, Badve C, Ponsky LE, Pahwa S, Dastmalchian S, Rogers M, Jiang Y, Margevicius S, Schluchter M, Tabayoyong W, Abouassaly R, McGivney D, Griswold MA, Gulani V. Development of a Combined MR Fingerprinting and Diffusion Examination for Prostate Cancer. Radiology 2017;283:729-38.
37. Sabouri S, Chang SD, Savdie R, Zhang J, Jones EC, Goldenberg SL, Black PC, Kozlowski P. Luminal Water Imaging: A New MR Imaging T2 Mapping Technique for Prostate Cancer Diagnosis. Radiology 2017;284:451-9.
38. Liney GP, Turnbull LW, Lowry M, Turnbull LS, Knowles AJ, Horsman A. In vivo quantification of citrate concentration and water T2 relaxation time of the pathologic prostate gland using 1H MRS and MRI. Magn Reson Imaging 1997;15:1177-86.

39. Arita Y, Takahara T, Yoshida S, Kwee TC, Yajima S, Ishii C, Ishii R, Okuda S, Jinzaki M, Fujii Y. Quantitative Assessment of Bone Metastasis in Prostate Cancer Using Synthetic Magnetic Resonance Imaging. Invest Radiol 2019;54:638-44.
40. Niu XK, Li J, Das SK, Xiong Y, Yang CB, Peng T. Developing a nomogram based on multiparametric magnetic resonance imaging for forecasting high-grade prostate cancer to reduce unnecessary biopsies within the prostate-specific antigen gray zone. BMC Med Imaging 2017;17:11.
41. Ding Z, Wu H, Song D, Tian H, Ye X, Liang W, Jiao Y, Hu J, Xu J, Dong F. Development and validation of a nomogram for predicting prostate cancer in men with prostate-specific antigen grey zone based on retrospective analysis of clinical and multi-parameter magnetic resonance imaging/transrectal ultrasound fusion-derived data. Transl Androl Urol 2020;9:2179-91.
42. Yang J, Li J, Xiao L, Zhou M, Fang Z, Cai Y, Tang Y, Hu S. (68)Ga-PSMA PET/CT-based multivariate model for highly accurate and noninvasive diagnosis of clinically significant prostate cancer in the PSA gray zone. Cancer Imaging 2023;23:81.
43. Beatrici E, Frego N, Chiarelli G, Sordelli F, Mancon S, Saitta C, De Carne F, Garofano G, Arena P, Avolio PP, Gobbo A, Uleri A, Contieri R, Paciotti M, Lazzeri M, Hurle R, Casale P, Buffi NM, Lughezzani G. A Comparative Evaluation of Multiparametric Magnetic Resonance Imaging and Micro-Ultrasound for the Detection of Clinically Significant Prostate Cancer in Patients with Prior Negative Biopsies. Diagnostics (Basel) 2024.
44. Wang Y, Wang W, Yi N, Jiang L, Yin X, Zhou W, Wang L. Detection of intermediate- and high-risk prostate cancer with biparametric magnetic resonance imaging: a systematic review and meta-analysis. Quant Imaging Med Surg 2023;13:2791-806.
45. Enikeev D, Morozov A, Taratkin M, Barret E, Kozlov V, Singla N, Rivas JG, Podoinitsin A, Margulis V, Glybochko P. Active Surveillance for Intermediate-Risk Prostate Cancer: Systematic Review and Meta-analysis of Current Protocols and Outcomes. Clin Genitourin Cancer 2020;18:e739-53.

Cite this article as: Cao W, Lin J, Chen Y, Ling J, Meng T, Wen Z, Xie C, Qian L, Guo Y, Zhang W, Wang H. Cancer detection in patients with prostate-specific antigen levels within the grey zone: can synthetic magnetic resonance imaging aid in the differentiation between prostate cancer and noncancerous lesions? Quant Imaging Med Surg 2024;14(12):9157-9168. doi: 10.21037/qims-24-1014

